ELSEVIER

European Journal of Radiology 59 (2006) 149–156

EJR
EUROPEAN JOURNAL OF RADIOLOGY

www.elsevier.com/locate/ejrad

Pre-clinical testing of a phased array ultrasound system for MRI-guided noninvasive surgery of the brain—A primate study

Kullervo Hynynen [a,*], Nathan McDannold [a], Greg Clement [a], Ferenc A. Jolesz [a], Eyal Zadicario [b], Ron Killiany [c], Tara Moore [c], Douglas Rosen [c]

[a] *Department of Radiology, Brigham and Women's Hospital and Harvard Medical School, 75 Francis Street, Boston, MA 02115, USA*
[b] *InSightec, Inc., Haifa, Israel*
[c] *Boston University, Boston, MA, USA*

Received 4 April 2005; received in revised form 5 April 2006; accepted 7 April 2006

Abstract

MRI-guided and monitored focused ultrasound thermal surgery of brain through intact skull was tested in three rhesus monkeys. The aim of this study was to determine the amount of skull heating in an animal model with a head shape similar to that of a human. The ultrasound beam was generated by a 512 channel phased array system (Exablate® 3000, InSightec, Haifa, Israel) that was integrated within a 1.5-T MR-scanner. The skin was pre-cooled by degassed temperature controlled water circulating between the array surface and the skin. Skull surface temperature was measured with invasive thermocouple probes. The results showed that by applying surface cooling the skin and skull surface can be protected, and that the brain surface temperature becomes the limiting factor. The MRI thermometry was shown to be useful in detecting the tissue temperature distribution next to the bone, and it should be used to monitor the brain surface temperature. The acoustic intensity values during the 20 s sonications were adequate for thermal ablation in the human brain provided that surface cooling is used.

Keywords: Ultrasound; High-intensity focused thermal ablation; Brain; MRI; Ultrasound surgery

1. Introduction

Applying focused ultrasound surgery in the brain has been hampered by the presence of the skull, which distorts the ultrasound beam due to its variable thickness and high sound speed [1]. In addition the skull causes excessive tissue temperatures as a result of its high acoustic attenuation coefficient [2]. For this reason clinical ultrasound surgery of brain tissues has only been explored through an acoustic window that was created by removing a piece of bone [3,4]. Although low frequency focusing of ultrasound through some locations of human skull was shown to be feasible [5], noninvasive brain surgery has not been explored until several key advances that occurred in recent years. First, it was demonstrated that large area phased arrays can be used to correct the beam distortion induced by the skull [6]. This and a series of numerical simulations [7] have led to the development of large hemispherical arrays [8] that maximize the focusing gain and thus minimize the skull heating. Second, a noninvasive method that uses CT-derived information to correct for wave distortion was developed and tested [9]. Based on these studies, an experimental system (ExAblate® 3000, InSightec, Haifa, Israel) was designed for pre-clinical application and tested with *ex vivo* human skulls and *in vivo* rabbit brains [10]. In this paper, the system was further tested in primates to establish the clinical feasibility of the approach. Due to the small size of the primate head, which limited the exposure levels that we could apply, these experiments were designed to establish the maximum intensity levels that could be delivered through the living skull bone.

2. Methods

2.1. Sonication system

Based on ex vivo human skull [11] and animal experiments [10] a clinical prototype ultrasound system was developed (ExAblate® 3000). This system consisted of a hemispherical ultrasound array with 512 equal area elements and a radius

* Corresponding author. Tel.: +1 617 278 0606; fax: +1 617 278 0610.
E-mail address: kullervo@bwh.harvard.edu (K. Hynynen).

0720-048X/$ – see front matter © 2006 Elsevier Ireland Ltd. All rights reserved.
doi:10.1016/j.ejrad.2006.04.007

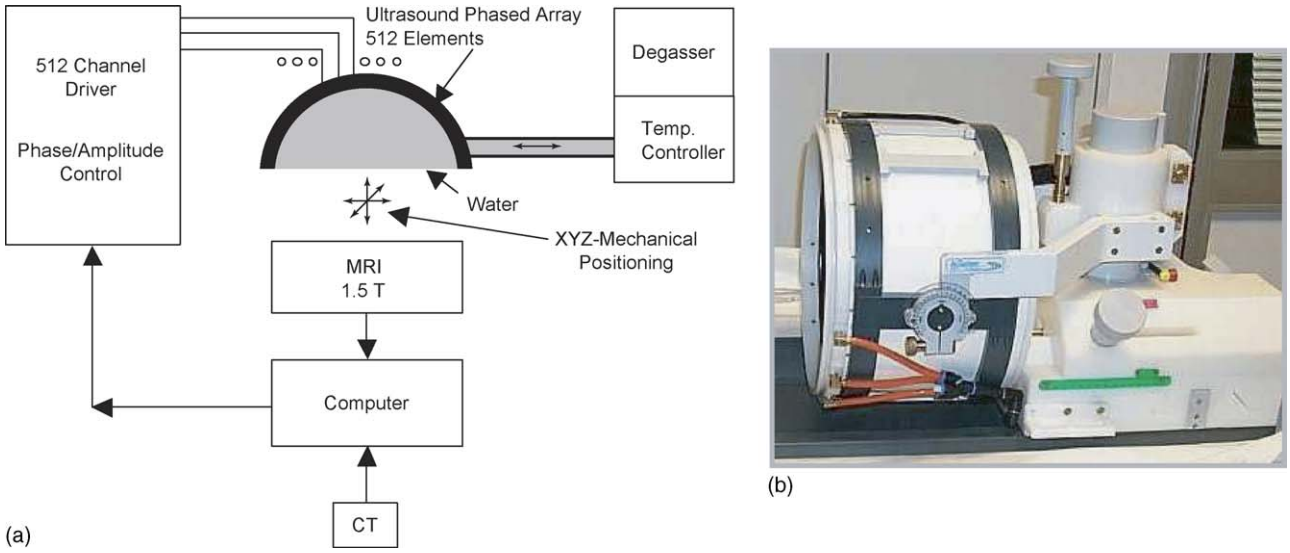

Fig. 1. (a and b) A diagram of the complete sonication system and a photograph of the array and the manual positioning mechanism.

of curvature of 15 cm (frequency = 670 kHz, manufactured by Imasonic, Besancon, France). Each of the array elements were driven with a separate RF line with independent amplitude and phase control. The multi-channel RF driver was under computer control. The hemispherical array was positioned on its side and connected to a three dimensional manual positioning device that allowed the array to be aimed in the target volume (Fig. 1a and b).

2.2. Animals

The MRI-guided focused ultrasound system was tested in three rhesus monkeys. The animals were anesthetized with a mix of ketamine (10 mg/kg) and xylazine (1.25 mg/kg) prior to the experiments. The hair on the head of each monkey was removed with clippers and hair-removing lotion prior to the experiments. The animal was positioned on its back, and its head was held in place with an acrylic holder so that the brain was centered in the ultrasound array. The head was inserted through a hole in a latex membrane that was slightly smaller in diameter of the head. The membrane was secured to the edges of the array thereby creating a watertight compartment between the array surface, the membrane, and the skin on the head. This space was filled with temperature controlled, degassed, circulating water to both couple the ultrasound to the head and to cool the skin and skull. During the first experiments, it was observed that the latex membrane used to couple the head to the array restricted the motion of the array with respect to the head. The membrane was so tight that when the array was moved, it also shifted the head. Since immobilization and registration of the head is critical, it was determined that a new design was required to allow

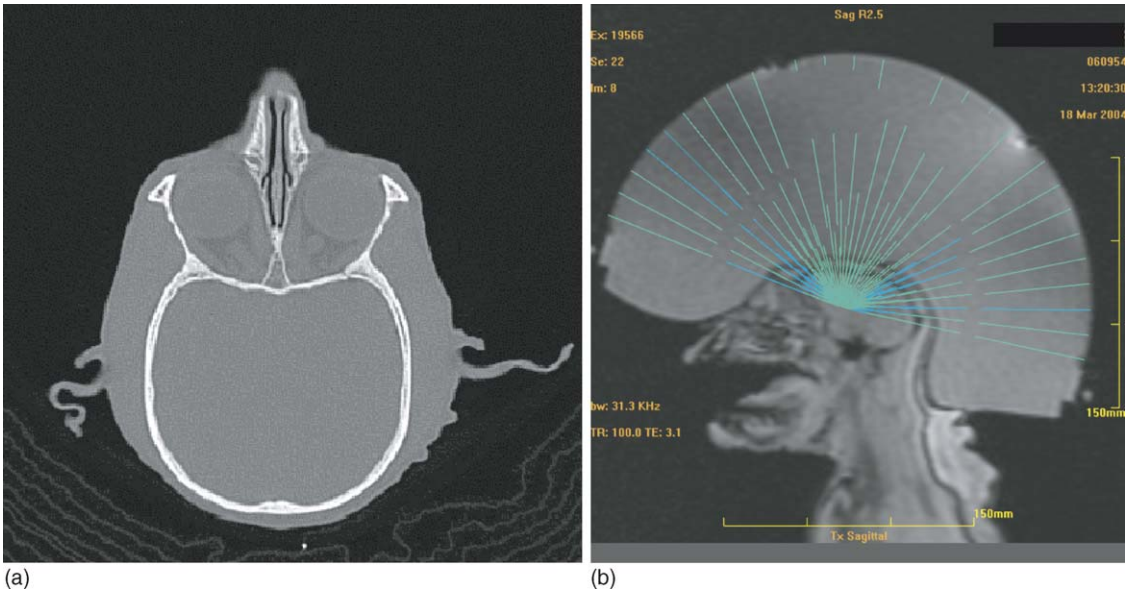

Fig. 2. (A) An axial CT-scan of one of the monkeys showing the skull bone. (B) MR-imaging of one animal placed within the ultrasound array with the central lines of each ultrasound beam superimposed on T2-weighted sagittal FSE image as illustrated in the figure. The various distances from the array elements to the skull surface are demonstrated by the length of the green and blue-colored lines.

the transducer array to be freely moved to target the desired locations. A new membrane was designed by InSightec to allow better lateral motion and it was used in the last animal experiment. The animals were sacrificed after the sonications, and a necropsy was performed.

2.3. Sonications

Prior to the sonications, each animal was imaged with a Siemens SOMATOM CT Scanner (FOV = 20 cm, slice thickness = 1 mm). A bone reconstruction kernel was used to acquire image intensities proportional to the bone density (Fig. 2A). In the beginning of the experiments, the array position was imaged using either Fast Spin Echo (FSE) or Gradient Echo (GE) images (Table 1). The images showed the array outline with markers that allowed the location of the geometric focal spot to be determined from the images. Then the animal head was imaged with three orthogonal sets of T2-weighted FSE images (Table 1) to localize the head and the skull. The CT and MRI images were co-registeredby using an overlay display that allowed visual inspection and manual alignment. This procedure made it possible for the system to use the CT information of the bone shape and density in the ultrasound propagation algorithm to determine the driving signal (amplitude and phase) for each transducer element to achieve a well-focused beam through the skull [9]. In addition, this identification of the skull bone allowed the system to determine the entrance angle of the beam for each transducer element (Fig. 2B).

The target location was selected from the MR images. To target the desired location, the array was mechanically moved with respect to the head's position. This targeting was accomplished by three manual lead screw sliders in the array holder. The sonications were performed while acquiring MR temperature images in planes oriented along the focus. The 20 s sonications were delivered at a frequency of 0.67 MHz [8] with acoustic powers between 20 and 300 W. A total of 28 sonications were performed in these monkeys. The sonications in the first monkey were performed with uniform intensity emitted from the array elements. The next two monkeys were sonicated so that a uniform intensity was incident across the skull surface.

In the second and third animal, thermocouple probes were inserted under the skin so that the sensors were adjacent to the skull bone. The thermocouples were in-house manufactured by twisting 0.05 mm diameter copper and constantan wires (California Fine Wire Co., Grover Beach, CA). The junction was soldered and left bare to avoid artifacts induced by the sonications.

Experiments were performed by focusing the beam in various locations within the brain while imaging the temperature elevation with the MRI. Temperature images were acquired in one plane from phase-difference images of a fast spoiled gradient echo sequence (3) (Table 1). A temperature sensitivity of −0.010 ppm/°C was used [12]. The temperature history was used to calculate the thermal dose with the formula proposed by Sapareto and Dewey [13].

3. Results

The MRI thermometry acquired during sonications in the first monkey revealed a non-uniform temperature distribution on the

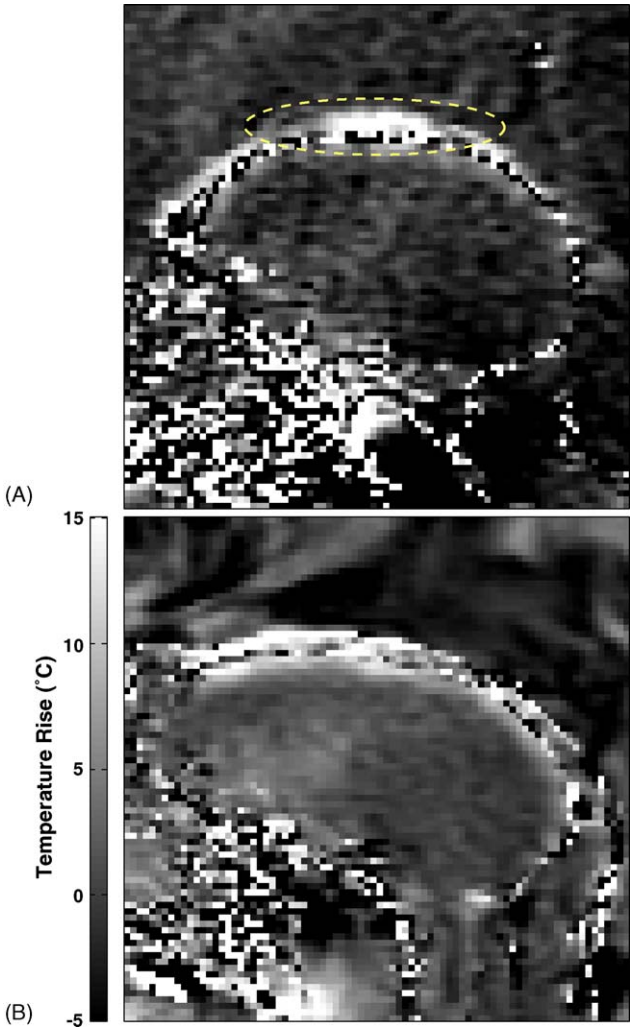

Fig. 3. The MRI thermometry image after 20 s heating showing the temperature distribution around the skull in the first two monkeys. (A) Uniform ultrasound intensity was used at the array surface. The ellipse enclosed the hot spot induced by non-uniform skull surface intensity. (B) Uniform ultrasound intensity was used at the outer surface of the skull.

Table 1
Parameters used in the MR imaging

Sequence	TR (ms)	TE (ms)	Flip angle (°)	Echo train length	Field of view (cm)	Matrix size	Slice thickness (mm)	Bandwidth (kHz)	NEX
T2-weighted FSE (planning)	2000	80	90	8	24	256 × 256	3	31	2
Gradient echo (planning)	100	5.4	30	N/A	24	256 × 256	3	31	1
FSPGR (temperature)	38.4	19.1	30	N/A	32	256 × 128	5 or 10	3.6	1

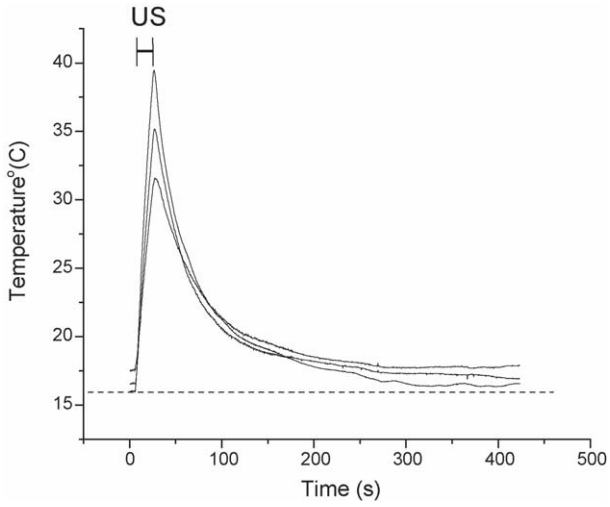

Fig. 4. Temperature–time curves of three thermocouple probes inserted under the skin and on the skull in one experiments. The initial temperature of 16–17.5 °C was reached after the circulating water temperature was circulating at approximately 12 °C. The rectal temperature of the animal was 33.3 °C. The average sonication intensity at the skull surface was approximately 3 W/cm^2 and the duration of the sonication was 20 s.

skull surface (Fig. 3A). This outcome was due to the asymmetric shape of the skull and the variable distance between the skull bone and the surface of the transducer array. This resulted in a variable intensity, and thus a non-uniform temperature rise at the bone surface. To avoid uneven heating, the ablation system was upgraded to have an operating mode that allowed the distance between the skull and the array elements to be taken into account so that a uniform intensity was delivered on the bone surface (Fig. 2B). In the second and third experiment, this operating mode was used, and a more uniform temperature elevation was observed on the skull surface (Fig. 3B). Since this functionality was not available in the first experiment, only the last two experiments will be analyzed in detail for the skull heating.

The thermocouples on the skull showed that the circulating water temperature (approximately 12 °C) reduced the skull surface temperature to 16–18 °C. During the 20 s sonication the bone surface temperature increased proportionally to the applied acoustic intensity and then returned to the baseline within approximately 5–7 min after sonication (Fig. 4). The thermocouple probes measured a maximum temperature elevation of approximately 8 °C/W/cm^2 on the outer skull surface. The average temperature elevation over all of the probes and sonications was 6 ± 2 °C/W/cm^2. The MRI measurements using the ten hottest voxels of those that neighbored the skull in the image plane resulted in an average slope of 6.6 ± 0.7 °C/W/cm^2. The average temperature rise over the entire heated skull surface was 4.5 ± 0.4 °C/W/cm^2 (Fig. 5).

The brain surface temperature also increased during the sonications, as determined by the MRI thermometry. The average temperature elevation over the brain surface for all sonications for both animals as plotted in Fig. 5 was 2.6 ± 0.2 and 4.0 ± 0.2 °C/W/cm^2 when just the 10 hottest voxels were analyzed. The brain surface temperature decayed to approximately half of its peak value approximately at two min after the end of the sonications (Fig. 6A). The temperature elevation decreased rapidly as a function of depth (Fig. 6B) such that the temperature elevation was reduced to 50% of the surface value at a depth of 2 mm.

Thermal dose maps were then calculated from the time history of temperature maps. The thermal dose is an index that

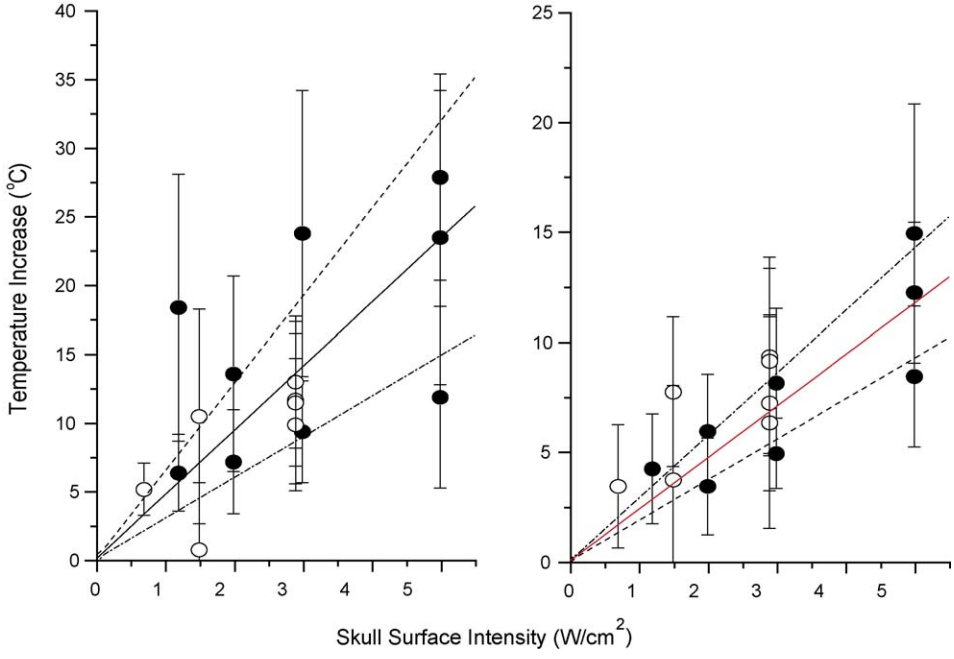

Fig. 5. The MRI thermometry derived average temperature increase (±S.D.) in the soft tissues just on the skull surface (left) and on the brain surface (right). These measurements included all of the voxels during MR-thermometry next to the skull over the area where temperature elevation was observed.

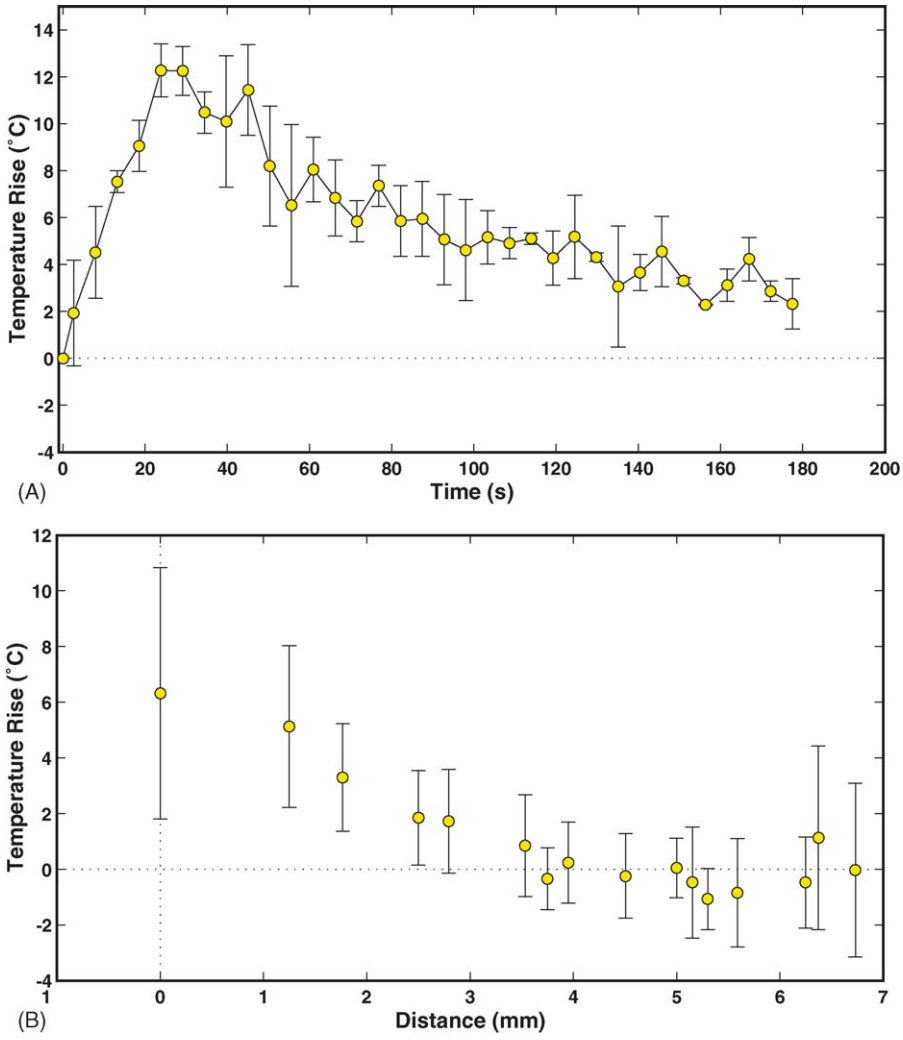

Fig. 6. (A) The brain surface temperature elevation derived from the MRI thermometry as a function of time. The temperature maps had motion artifacts that were corrected using three reference locations outside of the heated volume. (B) The temperature elevation at the end of the sonication as a function of the depth in the brain.

takes both the temperature and the time into account and has been shown to correlate well with the onset for tissue damage. Fig. 7 shows coronal dose maps of the brain, which was outlined. The gray color indicates regions that reached 17.5-equivalent minutes at 43 °C. A dose of 17.5 min has been shown to be the value where the probability for thermal brain damage is approximately 50% [14]. The post-mortem evaluation of the brain revealed several discolored spots on the brain surface (Fig. 7B) that indicated thermal coagulation of the tissue. These locations correlated with hottest regions and pixels in the dose maps, predicted by the MRI thermometry in the imaging planes, indicating damage in discrete areas at the top and sides of the head.

The cumulative thermal exposure of all of the sonications for the third animal was also calculated and is shown in Fig. 7C when intensities up to 3 W/cm^2 were used. This figure shows that at the accumulated thermal exposure was not enough to cause tissue damage on the brain surface. Gross inspection of the brain surface after the experiments did not show any damage (Fig. 7D).

4. Discussion

These results continue to support our earlier hypothesis [6], as well as in vivo rabbit brain sonications through ex vivo human skulls [10], and simulation studies [2,7] that ultrasound induced, completely noninvasive, thermal ablation of human brain tissue may be feasible. From these results, however, it appears that cooling of the coupling water is required in order to keep the outer skull surface temperatures within an acceptable range.

4.1. Skin and skull surface cooling

The experiments demonstrate the importance to perform sonications so that the ultrasound intensity on the bone surface is uniform, thus reducing the potential for power-limiting hot spots on the skull surface. The skin and the outer skull surface were further protected by the cooling of the circulating water. A skull surface temperature of 16–18 °C was measured when the water was cooled to approximately 12 °C. By cooling the skull

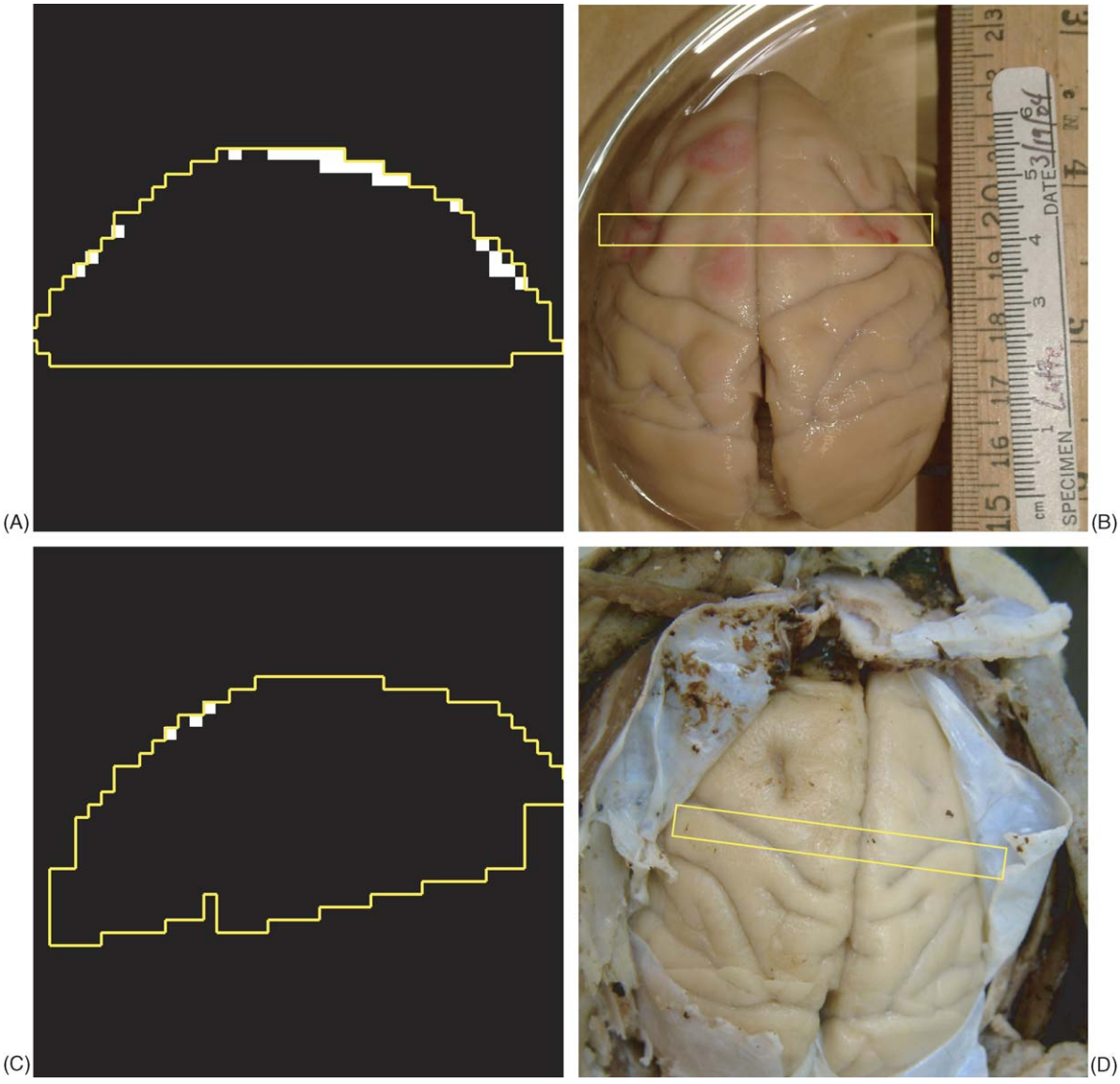

Fig. 7. The MRI thermometry derived thermal dose maps in coronal plane and photographs of the brain surface of the two animals that had sonications with uniform skull surface intensity. (A and B) Animal no. 2 with sonications up to 5 W/cm^2 surface intensity and one sonication where the animal moved increasing the intensity at the skull. The thermal dose map shows above threshold doses in several areas, and the photograph shows clear thermal damage on the brain surface (reddish colored areas). (C and D) Animal no. 3 that was sonicated at intensities up to 3 W/cm^2. Only a few voxel shows above the threshold dose and the photographs shows normal brain surface. The body temperature of this animal was measured with a rectal probe to be approximately 33 °C and thus the baseline brain surface temperature was estimated to be approximately 30 °C based on our simulation study [2]. The approximative location of the temperature monitoring image is indicated on the brain photographs.

surface and skin, for example to 17 °C, the sonication could increase the skull temperature by 25 °C without inducing undesired effects (absolute temperature <42 °C). The thermocouple probes measured a maximum temperature elevation of approximately 8 °C/W/cm^2, and the MRI measurements using the ten hottest pixels gave an average slope of 6.6 ± 0.7 °C/W/cm^2. When all of the voxels next to the skull were used an average temperature rise over the heated skull surface of 4.5 ± 0.4 °C/W/cm^2 was detected. In pig experiments [15] the average skull surface temperature elevation was 3.4 ± 1.1 °C/W/cm^2 indicating that the primate skull may absorb higher levels of the energy transmitted by ultrasound.

4.2. Brain surface

The outer surface of the brain also heated up due to the energy absorption in the bone. The slope of the fitted data gave a temperature elevation across the brain surface of 2.6 ± 0.2 °C/W/cm^2 with the hottest voxels giving an average value of 4.0 ± 0.2 °C/W/cm^2. In similar pig experiments [15] the average brain surface heating was observed to be 2.2 ± 0.5 °C/W/cm^2, again demonstrating a slight difference between a primate and pig skull. If 42 °C were used as the limit for the brain temperature then 1.25 W/cm^2 would be the intensity limit for the 20 sonications. Since this heating is localized

close to the brain surface the impact of the temperature elevation could be reduced by cooling the brain surface. Based on our simulation study [2] the cooling of the skin will extend into the brain. In the simulations, a 15 °C skin surface temperature was able to reduce the skull inner surface temperature (and thus the brain surface temperature) to 34 °C. In these simulations, the skull temperature had not yet reached a steady state and thus even lower temperatures could be expected. There is also experimental evidence of reaching brain temperature of 34 °C from brain injury studies where scalp cooling was explored [16]. Therefore, even in the most aggressive cooling situation the temperature elevation on the brain surface is the intensity limiting factor for transcranial sonications.

4.3. Human treatments

Due to the small size of the monkey brain, the focal spot distance from the skull was as low as approximately 20 mm or less. Thus, it was not possible to induce brain tissue coagulation at the focus without overheating the brain surface. Based on the temperature elevation measured, it can be predicted that an acoustic power of approximately 600 W would be required to elevate the focal temperature above the tissue coagulation threshold. An intensity of for example 2 W/cm^2 for 20 s would provide a total acoustic power to approximately 1000 W if a surface area of 500 cm^2 would have been covered [17]. One should note that the brain surface cools relatively slowly after ultrasound exposures and thus, careful selection of adequate sonication intervals is mandatory when multiple sonications are used.

In two of the three animals, the post-mortem evaluation showed several spots of thermally coagulated tissue on the outer brain surface. In the first animal, the damaged tissue correlated with excessive thermal dose on the brain surface during the high power sonications and uneven intensity distribution. In the second animal, the thermal dose analysis of the temperature images demonstrated that the damage could be correlated to the first sonication when the animal moved and the focus-to-bone distance was less than 10 mm. The thermal dose maps of the third animal did not show any areas that received a thermal dose above the threshold for damage. This finding was verified in the post-mortem examination, indicating that the MRI thermometry was a reliable predictor of the tissue damage and that on-line MRI thermometry should be used for monitoring and control of the patient treatments to assure safety. However, this requires knowledge of the baseline temperature of the tissue which is not yet well known during extensive skin cooling. For our thermal dose calculation in these monkeys, we used an estimate of brain surface temperature of 30 °C due to the aggressive skin cooling and measured body temperature of approximately 33 °C. Based on the thermal dose maps it was possible to use skull surface intensity up to 3.0 W/cm^2 without evidence of lethal dose values on the brain surface. It should be noted that since there often is excess noise in the MRI temperature maps right at the surface due to the effects of the neighboring bone, it is possible that these voxels were influenced by noise.

Skull heating limits the ultrasound power available for the focal tissue coagulation and may prevent coagulation of locations close to skull with a single sonication. A multi-sonication approach has been shown to reduce limitation of sonication power and the resulting skull heating [18]. The skull heating can be further reduced using gas bubble enhanced heating [19,20] or direct mechanical tissue destruction induced by cavitation [21] since both of these methods can reduce the time average power required. The applied ultrasound power can be further reduced by using preformed gas bubbles injected in the blood stream to enhance the heating and tissue damage [22,23]. Focal surgery of brain tumors may also be possible by using the ultrasound to release drugs from temperature sensitive carriers [24] at low temperatures or using the focused beam to disrupt the blood–brain barrier for the delivery of toxic molecules that could selectively target the brain cells [25]. This method may allow also molecular delivery for the treatment of many brain dysfunctions beyond surgery. All of the above approaches will require lower skull surface intensities than the thermal coagulation of brain tissue and thus, they should be feasible with the method described here.

So far, focused ultrasound was also used with an invasive hydrophone to aid in the focusing through the skulls of sheep [26]. Those experiments showed focal lesions without significant side effects in an animal brain. This group used cooling of the skull but did not measure the skull surface temperatures. Based on our experiments, the skull heating should have been a problem with in the experiments if purely thermal tissue coagulation was used. However, the insertion of a hydrophone in the brain will introduce gas and can enhance the temperature elevation, so a direct comparison between their results and those presented in this paper may not be possible.

Due to the small size of the head of the monkeys, our experiments could not test the focusing ability of the system. Ex vivo human skulls have shown that a propagation algorithm that takes the CT derived bone density into account will provide reliable focusing through human skulls [9]. A similar method has also been proposed and tested by others [27]. However, clinical trials are ultimately required to determine if the ex vivo human skull derived speed of sound [28] and attenuation values [2] are accurate enough for the proposed work.

Acknowledgements

This research was supported by a research grant and equipment from InSightec, Haifa, Israel, and by NIH grant EB003268.

References

[1] Fry FJ, Barger JE. Acoustic properties of the human skull. J Acoust Soc Am 1978;63:1576–90.
[2] Connor CW, Hynynen K. Patterns of thermal deposition in the skull during transcranial focused ultrasound surgery. IEEE Trans Biomed Eng October 2004;51(10):1693–706.
[3] Fry WJ, Fry FJ. Fundamental neurological research and human neurosurgery using intense ultrasound. IRE Trans Med Electron July 1960;ME-7:166–81.
[4] Heimburger RF. Ultrasound augmentation of central nervous system tumor therapy. Indiana Med 1985;78:469–76.
[5] Fry FJ, Goss SA, Patrick JT. Transkull focal lesions in cat brain by ultrasound. J Neurosurg 1981;54(5):659–63.

[6] Hynynen K, Jolesz FA. Demonstration of potential noninvasive ultrasound brain therapy through intact skull. Ultrasound Med Biol 1998;24(2):275–83.
[7] Sun J, Hynynen K. Focusing of ultrasound through a human skull: a numerical study. J Acoust Soc Am 1998;104(3):1705–15.
[8] Clement GT, Sun J, Giesecke T, Hynynen K. A hemisphere array for non-invasive ultrasound brain therapy and surgery. Phys Med Biol Jan 2000;45(12):3707–19.
[9] Clement GT, Hynynen K. A non-invasive method for focusing ultrasound through the human skull. Phys Med Biol April 2002;47(8):1219–36.
[10] Hnynen K, Clement GT, McDannold N, et al. 500-Element ultrasound phased array system for noninvasive focal surgery of the brain: A preliminary rabbit study with ex vivo human skulls. Magn Reson Med July 2004;52(1):100–7.
[11] Clement GT, White PJ, King RL, McDannold N, Hynynen K. A magnetic resonance imaging-compatible, large-scale array for transskull ultrasound surgery and therapy. J Ultrasound Med August 2005;24(8):1117–25.
[12] Vykhodtseva N, King R, White PJ, Vitek S, Jolesz FA. 500-Element ultrasound phased array system for noninvasive focal surgery of the brain: a preliminary rabbit study with ex vivo human skulls. Magn Reson Med July 2004;52(1):100–7.
[13] Sapareto SA, Dewey WC. Thermal dose determination in cancer therapy. Int J Radiat Oncol Biol Phys 1984;10:787–800.
[14] McDannold N, Vykhodtseva N, Jolesz FA, Hynynen K. MRI investigation of the threshold for thermally induced blood–brain barrier disruption and brain tissue damage in the rabbit brain. Magn Reson Med May 2004;51(5):913–23.
[15] McDannold N, King RL, Hynynen K. MRI monitoring of heating produced by ultrasound absorption in the skull: in vivo study in pigs. Magn Reson Med May 2004;51(5):1061–5.
[16] Wang H, Olivero W, Lanzino G, et al. Rapid and selective cerebral hypothermia achieved using a cooling helmet. J Neurosurg February 2004;100(2):272–7.
[17] Sun J, Hynynen K. The potential of transskull ultrasound therapy and surgery using the maximum available skull surface area. J Acoust Soc Am 1998;104(4):2519–27.
[18] Yin, X, Hynynen K. A numerical study of pulsed sonication for reducing thermal deposition in the skull during transcranial focused ultrasound surgery. Proceedings of IEEE Ultrasonics Symposium, 2005, 1241–44.
[19] Sokka SD, King R, Hynynen K. MRI-guided gas bubble enhanced ultrasound heating in in vivo rabbit thigh. Phys Med Biol January 2003;48(2):223–41.
[20] Curiel L, Chavrier F, Gignoux B, Pichardo S, Chesnais S, Chapelon JY. Experimental evaluation of lesion prediction modelling in the presence of cavitation bubbles: intended for high-intensity focused ultrasound prostate treatment. Med Biol Eng Comput 2004;42(1):44–54.
[21] Vykhodtseva NI, Hynynen K, Damianou C. Histologic effects of high intensity pulsed ultrasound exposure with subharmonic emission in rabbit brain in vivo. Ultrasound Med Biol 1995;21(7):969–79.
[22] Simon RH, Ho SY, Lange SC, Uphoff DF, D'Arrigo JS. Applications of lipid-coated microbubble ultrasonic contrast to tumor therapy. Ultrasound Med Biol 1993;19(2):123–5.
[23] Hynynen K, McDannold N, Martin H, Jolesz FA, Vykhodtseva N. The threshold for brain damage in rabbits induced by bursts of ultrasound in the presence of an ultrasound contrast agent (Optison). Ultrasound Med Biol March 2003;29(3):473–81.
[24] Needham D, Anyarambhatla G, Kong G, Dewhirst MW. A new temperature-sensitive liposome for use with mild hyperthermia: characterization and testing in a human tumor xenograft model. Cancer Res March 2000;60(5):1197–201.
[25] Hynynen K, McDannold N, Vykhodtseva N, Jolesz FA. Noninvasive MR imaging-guided focal opening of the blood–brain barrier in rabbits. Radiology Sept 2001;220(3):640–6.
[26] Pernot M, Aubry JF, Tanter M, Boch AL, Kujas M, Fink M. Adaptive focusing for ultrasonic transcranial brain therapy: first in vivo investigation on 22 sheep. AIP Conf Proc March 2005;754(1):174–7.
[27] Aubry JF, Tanter M, Pernot M, Thomas JL, Fink M. Experimental demonstration of noninvasive transskull adaptive focusing based on prior computed tomography scans. J Acoust Soc Am January 2003;113(1):84–93.
[28] Connor CW, Clement GT, Hynynen K. A unified model for the speed of sound in cranial bone based on genetic algorithm optimization. Phys Med Biol Nov 2002;47(22):3925–44.